Rheol Acta (2001) 40: 426–433

ORIGINAL CONTRIBUTION

J. Adrian Reyes
Octavio Manero
Rosalio F. Rodríguez

Electrorheology of nematic liquid crystals in uniform shear flow

Received: 23 November 1999
Accepted: 13 June 2000

J. A. Reyes · R. F. Rodríguez (✉)
Instituto de Física, Universidad Nacional Autónoma de México
Apdo. Postal 20–364
01000 México, D.F., México
e-mail: zepeda@fenix.ifisicacu.unam.mx

O. Manero
Instituto de Investigaciones en Materiales
Universidad Nacional Autónoma de México, Apdo. Postal 70–360
01000 México, D.F., México

Abstract A hydrodynamic model for the electrorheological effect in a polymeric nematic confined in a rectangular cell is studied. The competition between a constant electric and a uniform shear flow is explicitly considered. For the final stationary state where the induced reorientation of the director has already occurred, we show that the averaged viscosity is enhanced. For this same state several rheological properties such as the first normal stress difference and the force between the cell plates are also analytically calculated as a function of position, the applied field, and Reynolds' number. These results are compared with those obtained previously for a pressure driven flow. The scope and limitations of the model and methods employed are discussed.

Introduction

In a previous paper (Rodríguez et al. 1999) we have shown that liquid crystals are indeed interesting fluids for electrorheological applications (Tao 1992; Block and Kelly 1988). We studied a simple analytical model for the reorientation of a thin film of the polymeric nematic *poly*(*n-hexyl isocyanate*) (*PHIC*), when acted upon by an external electric field and an externally imposed plane Poiseuille flow on a liquid crystal planar cell with a separation of a few microns between its plates. We showed that the induced reorientation induced by both fields, produce an electrorheologic effect (*ER*), that is, an increase of almost three orders of magnitude in the apparent viscosity of *PHIC*. Our model shows that the reorientation of the nematic is the physical mechanism leading to the existence of the *ER* effect in this model. This same material was originally used by Yang and Shine (1992) to show the feasibility of liquid crystal systems to produce a practical *ER* in a rotational rheometer.

In this paper we consider the case of uniform flow. By assuming that director's reorientation in the presence of a constant electric field and flow is a relaxation process, we derive a coupled set of nonlinear hydrodynamic equations for the director and the velocity field (San Miguel and Sagués 1987; Rodríguez and Reyes 1995; Rodríguez et al. 1996). The equation for the stationary orientational profile is solved in an approximate but analytical way by using boundary layer methods. Using this solution the apparent (orientational) viscosity is calculated and plotted as a function of the dimensionless external field for different values of the Reynold's number. As in Rodríguez et al. (1999), this curve shows a large increase in the viscosity (*ER*). It is also shown that the *ER* vanishes when a critical value of the Mason number, M_a^c, is exceeded. Our analytical approach allows us to calculate this critical value and express it in terms of material properties and flow parameters. Some rheological properties are then calculated in terms of the orientational profile, for instance, the stress tensor as a function of the flow strength; the first normal stress difference N_1 as a function of the position within the cell, the applied field and the Reynolds' number of the flow, and the force f between the plates of the cell as a function of the Reynolds number for different values of the electric field. We find that, in

contrast to the observed behavior of N_1 for plane Poiseuille flow where N_1 presents regions of negative values (Rodríguez et al. 1999), for simple shear this situation does not arise for the considered values of electric field and flow shear rates. This would only be possible for a strong electric field and a weak flow, conditions which are not attainable within the present analytical approach. Then the force on the plates is also calculated as a function of the velocity gradient and for different electric field strengths. We find that the net force increases with the electric field and remains almost constant with the velocity gradient for high values of the electric field. However, for some values of the field the magnitude of the force decreases as the velocity gradient increases and vanishes for a definite value of the dimensionless shear rate. A similar behavior presents the shear stress, which shows a steep drop at around the same value of the shear rate. It is very interesting to note that f becomes zero only for a specific value of the ratio between shear rate and field strength. This critical ratio signals the limit of existence of the electrorheological effect, in such a way that it corresponds to a regime of complete alignment of the director with the velocity. Finally, we close the paper by discussing the limitations and advantages of our approach.

Model and governing equations

A quiescent nematic layer of thickness l is contained between two parallel conducting plates, as depicted in Fig. 1. The transverse dimensions of the cell, L, along the x and y axes are large compared to l, so that the cell has a large aspect ratio but a finite volume $V = L^2 l$. If the initial orientation of the director is planar, when an external d.c. electric field E is applied along the z direction, the director $\vec{n}$ will reorient inside the cell for values of $E > E_c$, where E_c is the critical field that has to be exceeded to initiate the reorientation. Owing to the low aspect ratio of the cell, it is reasonable to assume this reorientation occurs only in the x–z plane. If in order to simplify the description, spatial homogeneity in the x direction is assumed, then $\vec{n} = [\sin\theta(z,t),\ 0, \cos\theta(z,t)]$, where it is also assumed that the reorientation angle θ satisfies strong anchoring conditions at the plates:

$$\theta\left(z = \pm\frac{l}{2}\right) = \pm\frac{\pi}{2} \ . \tag{1}$$

In addition to the electric field we assume that the plates may move relative to each other to produce an uniform shear flow in the x–z plane and along the x direction (Fig. 1). Then the only relevant component of the velocity field is v_x which will be assumed to satisfy the following no-slip boundary conditions:

$$v_x\left(z = \pm\frac{l}{2}\right) = 0 \ . \tag{2}$$

As usual, the reorientation of the director will be considered to be an isothermal process and, therefore, its equilibrium states may be described in terms of the associated Helmholtz free energy functional, which for the assumed geometry and in MKS units takes the form (Khoo 1988)

$$F = \int_V \mathrm{d}V \left\{ \frac{K}{2}\left(\frac{\mathrm{d}\theta}{\mathrm{d}z}\right)^2 - \frac{E^2}{2}\varepsilon_0\left(\varepsilon_\perp + \varepsilon_a \cos^2\theta\right) + \frac{1}{2}\rho v_x^2(z) \right\} , \tag{3}$$

where in writing this expression the assumption of equal elastic constants for the splay, bend and twist elastic deformations, $K \equiv K_1 = K_2 = K_3$ has been made. Here $\varepsilon_a \equiv \varepsilon_\parallel - \varepsilon_\perp$ stands for the dielectric anisotropy of the nematic, ε_0 denotes the permittivity of the vacuum, and $\rho(z,t)$ denotes the local mass density of the fluid. The last term in this equation represents the contribution to F due to the uniform shear flow along the x direction.

Following the usual procedure to derive nematodynamic equations (de Gennes 1964; San Miguel and Sagués 1987) from Eq. (3) we arrive at the following set of coupled dynamical equations for θ and v_x (Rodríguez et al. 1996):

$$\frac{\partial\theta}{\partial t} = \frac{2}{\gamma_1}\frac{\delta F}{\delta\theta} - (1-\lambda)\cos\theta\frac{\partial v_x}{\partial z} \ , \tag{4}$$

$$\frac{\partial v_x}{\partial t} = \frac{v_3}{\rho}\frac{\partial^2 v_x}{\partial z^2} + \frac{\lambda - 1}{2\rho}\frac{\partial}{\partial z}\left[\frac{1}{\cos\theta}\frac{\delta F}{\delta\theta}\right] \ , \tag{5}$$

where the variational derivative $\delta F/\delta\theta$ is given explicitly by

$$\frac{\delta F}{\delta\theta} = K\frac{\mathrm{d}^2\theta}{\mathrm{d}z^2} - \frac{\varepsilon_0\varepsilon_a}{2}E^2\sin 2\theta \ . \tag{6}$$

In these equations γ_1, γ_2, v_3, with $\lambda \equiv \gamma_1/\gamma_2$, denote the various viscosity coefficients of the nematic.

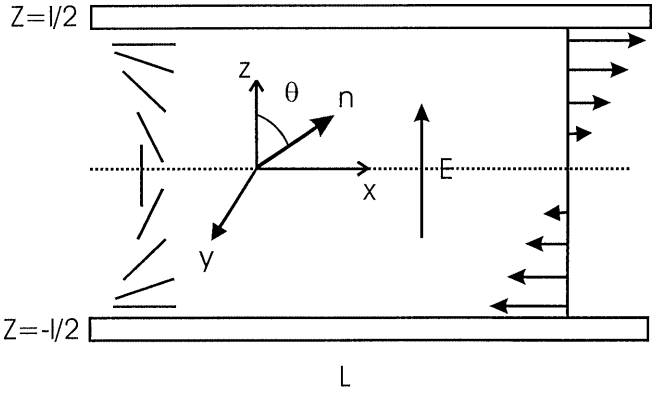

Fig. 1 Schematics of a planary aligned liquid crystal film in the presence of a constant electric field. The velocity profile of a uniform shear flow is also shown

Strictly speaking, Eqs. (4), (5), and (6) provide for a closed set of hydrodynamic equations for a low molecular weight nematic (thermotropic), since in this case the director is the only additional hydrodynamic variable, apart from the usual conserved variables of mass, specific entropy and momentum densities (Rodríguez and Reyes 1996). Since for a polymeric nematic (lyotropic) the corresponding description is much more involved owing to the large number of degrees of freedom that may contribute to the dynamics in the hydrodynamic limit, its complete formulation is still an open issue. Therefore, as a first approximation, we shall use the above formalism to describe the hydrodynamic behavior of a polymeric nematic solution of *PHIC*, as described by Yang and Shine (1992). It is important to stress that this is, indeed, a strong approximation; however, it is expected to be a reasonable one owing to the fact that molecular weight of *PHIC* ($\sim 10^5$) is not too large. If in addition the system is always away from a critical point, it is not necessary to account for the dynamics of an order parameter, which is not a hydrodynamic variable, and therefore its behavior can be described by considering the director field as the only additional hydrodynamic variable. This approximation has the great advantage of keeping the description simple enough so that an analytical treatment is possible and specific calculations can be carried out.

In this work we only consider the final stationary state characterized by the fact that the reorientation has already occurred, but flow effects are still present. For this case the calculation of some rheological properties, such as the viscometric functions, can be carried out explicitly (Rodríguez and Camacho 1998), as we shall see below. The final stationary state is defined by setting the left hand sides of Eqs. (4) and (5) equal to zero, which yields a closed equation for the final stationary orientational configuration. We shall carry out this procedure explicitly for a particular flow, namely, the uniform shear flow.

Uniform shear flow

This flow occurs when the plates move in opposite directions with constant velocity $\pm v_0$ in such a way that the velocity gradient $(\mathrm{d}v_x(\zeta)/\mathrm{d}\zeta) \equiv \dot{\gamma} = const$. In terms of the dimensionless variable $\zeta \equiv z/l$, Eq. (5) reduces to

$$\frac{\mathrm{d}^2 v_x}{\mathrm{d}\zeta^2} = 0 \ , \tag{7}$$

whose solution satisfying the boundary conditions $v_x(\zeta = \pm 1/2) = \pm v_0$ is given by $v_x = 2v_0\zeta/l$. By inserting this solution into the orientational equation (Eq. 4) we arrive at the following closed equation for θ:

$$\frac{\mathrm{d}^2\theta}{\mathrm{d}\zeta^2} + p\sin 2\theta - m\cos\theta = 0 \ , \tag{8}$$

with the dimensionless field strength

$$p \equiv q\bar{E}^2 \tag{9}$$

where

$$q \equiv \varepsilon_0\varepsilon_a E_c^2 l^2/2K \ , \tag{10}$$

and a dimensionless shear rate is given by

$$m \equiv R\gamma_1 v_3(1-\lambda)/\rho K \ . \tag{11}$$

Here $\bar{E} \equiv \frac{E}{E_c}$, where $E_c = \frac{\pi}{l}\sqrt{2K/\varepsilon_a\varepsilon_0}$ is the critical field (Khoo 1988) and is such that reorientation occurs if $\bar{E} > 1$. It is essential to emphasize that there are two important physical parameters in Eq. (8). On the one hand, p is proportional to the ratio between the energy of the incident field and the nematic's elastic energy. Therefore, it is a measure of the strength of the coupling between the external field and the induced orientational configuration. On the other hand, the parameter m, given by Eq. (11) contains the effects due to the hydrodynamic flow through the Reynolds number $R \equiv \rho v_0 l/v_3$.

Although the exact analytical solution of Eq. (8) can, in principle, be written in terms of elliptical functions, in this work we only shall consider its asymptotic solution for strong fields and large values of m. Thus, if we assume that $p \approx m \gg 1$, and follow the same boundary layer procedure sketched in Rodríguez et al. (1999), we find that the outer solution θ_{out} is given by Bender and Arszog (1978) and Schilchting (1968):

$$\theta_{out} = \arcsin\frac{m}{2p} \ . \tag{12}$$

To determine the inner solution note that the terms $p\sin 2\theta$ and $m\cos\theta$ are no longer dominant near the boundaries $\theta = \pm\pi/2$, where there should be boundary layers. Near these regions it is convenient to express the inner solution $\alpha \equiv \theta_{\mathrm{in}} \pm \pi/2$ in terms of the fast variable $\mu \equiv \sqrt{p}(\zeta \pm 1/2)$. For small values of α this leads to

$$\frac{\mathrm{d}^2\alpha}{\mathrm{d}\mu^2} - \sin 2\alpha \pm m/(2p)\sin\alpha = 0 \ . \tag{13}$$

The general solutions of this equation can be expressed as

$$\alpha = A\exp\left[\sqrt{2p - Sign[\zeta]m}|\zeta|\right] + B\exp\left[-\sqrt{2p - Sign[\zeta]m}|\zeta|\right] \ , \tag{14}$$

where A and B are arbitrary constants to be determined by the matching condition for the adjusted solution θ_{adj}:

$$\theta_{adj} = \theta_{out} + \theta_{in} - \theta_{match} \ . \tag{15}$$

If θ_{match} is calculated in such a way that $\theta_{out}(z)$ and $\theta_{in}(z)$ join asymptotically, and if the resulting expression together with θ_{out} and α are substituted into Eq. (15), we finally arrive at

$$\theta(\zeta;m,p) = \arcsin\left[\frac{m}{2p}\right] + \left(Sign[\zeta]\frac{\pi}{2} - \left[\frac{m}{2p}\right]\right) \frac{\sinh\left[\sqrt{2p - Sign[\zeta]m}\,|\zeta|\right]}{\sinh\left[\sqrt{2p - Sign[\zeta]m}/2\right]} \quad . \tag{16}$$

Notice from this equation that θ is continuous in the asymptotic limit of strong fields and flows, even though its first derivative is discontinuous. It is important to point out that this boundary layer method can be used only when the values of p and m are of the same order of magnitude, that is, when $\frac{m}{p} \sim 1$. Actually, for future reference it is convenient to express this ratio in terms of the Mason number, M_a, which is a measure of the relative magnitude of hydrodynamic and electrostatic forces. For the case of a simple shear flow it is defined as

$$M_a \equiv \frac{\eta_s \dot{\gamma}}{2\varepsilon_s(\beta E)^2} \quad , \tag{17}$$

where $\dot{\gamma}$ is the shear rate, η_s is the shear viscosity and E is the magnitude of the electrostatic field. β is the dipole coefficient defined as

$$\beta = \frac{\varepsilon_r - 1}{\varepsilon_r + 2} \quad , \tag{18}$$

being ε_r the dielectric constant ratio

$$\varepsilon_r = \frac{\varepsilon}{\varepsilon_s} \quad . \tag{19}$$

Here ε is the dielectric constant of the liquid crystal and ε_s is that of the solvent. Thus, it follows that

$$\frac{m}{p} = 4\frac{\gamma_1(1-\lambda)}{\nu_3}\frac{\varepsilon_s\beta^2}{\varepsilon_0\varepsilon_a}M_a \quad . \tag{20}$$

Note that M_a is expressed in terms of material properties and geometrical and flow parameters.

Results and discussion

Electrorheological effect

Let us consider first the orientational profile. Figure 2 illustrates a plot of the orientation angle θ vs ζ, as obtained from Eq. (16) for various values of the parameters m and p. θ presents a considerable increase in the region close to the walls, up to the boundary value of $p/2$. Notice that the orientation of the director is constant in most of the bulk central region of the cell, and its magnitude depends on the ratio m/p or Mason number. As the velocity gradient increases, i.e., as m increases, the orientation of the director tends to be more aligned with the direction of the fluid velocity in the central region of the cell. On the other hand, the electric field direction is normal to that of the flow, and therefore it opposes the alignment of the director with the flow direction. In the particular case when $p = m$, Eq. (16) implies that in the center of the cell the orientation is fixed to the value $\theta = \arcsin(1)$, meaning that the orientation angle at the center becomes multivalued. This multivalued solution implies that there are many different values of the velocity gradient and electric field compatible with the same orientation of the director at the channel center; in this sense it allows for a non-limited growth of the angle. The curve corresponding to $m = 160$, $p = 160$ in Fig. 2 also shows that $d\theta/d\zeta$ is discontinuous, although this is not noticeable in the other curves.

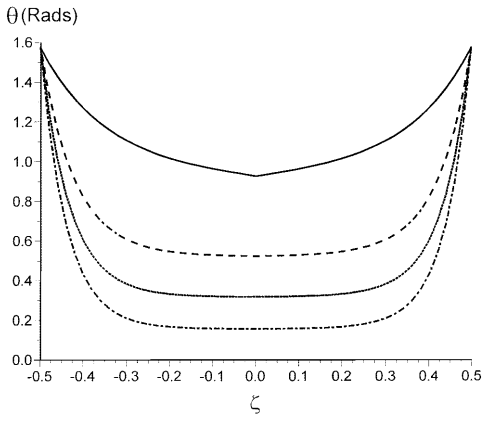

Fig. 2 Orientational configuration θ vs ζ of *PHIC* for different values as calculated from Eq. (16). (—) $m = 50$, $p = 160$; (–) $m = 100$, $p = 160$; (···) $m = 160$, $p = 160$; (–·–) $m = 160$, $p = 100$

It should be pointed out that the above result is in contrast to the one obtained in the case of Poiseuille flow where the orientation angle presents a sharp increase in a very narrow region around the central part of the channel and a small variation in the remaining of the cell; see Fig. 2 in Rodríguez et al. (1999). The orientation of the director is almost parallel to the walls in most of the cell and only in the cell's center, where the velocity gradient is zero, is aligned with the electric field. In contrast, in simple shear flow, where a constant velocity gradient is imposed, the orientation of the director changes rapidly and attains a specific value dependent on the ratio m/p in most of the central region. Only in the situation when this ratio is large, the orientation of the director remains almost parallel to the flow direction.

The apparent viscosity relates the shearing force per unit area with the magnitude of the local shear. Its dependence on the orientation of the director occurs through the expression (Carlsson 1984)

$$\eta(\theta(\zeta);\bar{E}) = \alpha_1 \cos^2\theta \sin^2\theta + \eta_c + (\alpha_2 + \alpha_3)\sin^2\theta \quad , \tag{21}$$

where α_1, α_2, α_3 are the Leslie coefficients, and η_c is the transverse Miesowicz viscosity (Miesowicz 1935). Since

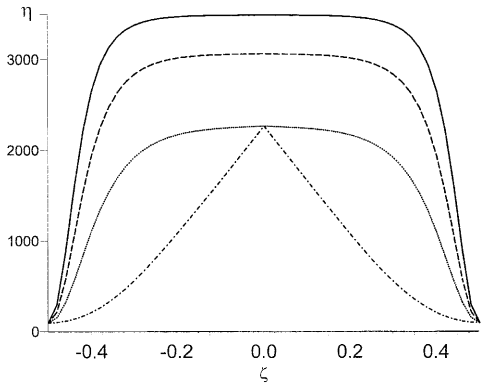

Fig. 3 Orientation viscosity η vs ζ as calculated from Eq. (17) for *PHIC*. (—) $m=50$, $p=160$; (–) $m=100$, $p=160$; (···) $m=160$, $p=160$; (·–) $m=10$, $p=10$

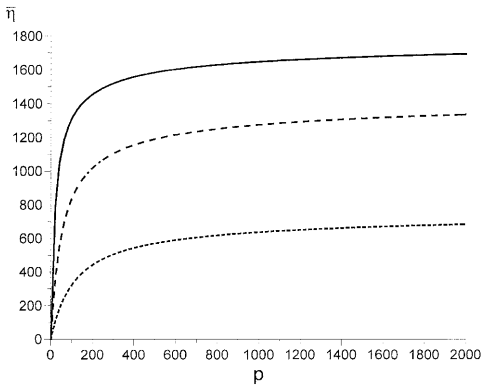

Fig. 4 Averaged viscosity $\bar{\eta}$ vs p parametrized by m/p. (—) $m/p=0.1$; (–) $m/p=1$; (···) $m/p=1.5$

the orientation angle θ is given by Eq. (16), the way in which η depends on θ indicates that the system is non-Newtonian, since η is strongly dependent on the driving force. From Eqs. (16) and (17) we obtain the spatial variation of η within the cell. Figure 3 shows a plot of $\eta[\theta(\zeta);\bar{E}]$ vs ζ, as given by Eq. (17), for different values of p and the non-dimensional velocity gradient m. The shear viscosity remains almost constant in most of the cell width and decreases towards the walls, giving rise to a narrow low-viscosity region next to them. The low viscosity region reflects the alignment of the director parallel to the flow direction in the neighborhood of the walls. The variation of the viscosity is sharper as the flow strength diminishes, since the electric field orientation (normal to the flow direction) dominates the director orientation as the ratio m/p decreases. On the other hand, when the flow dominates the director orientation, the viscosity diminishes as m increases; this is specially noticeable for $m=p=10$. This gives rise to a strong dependence of the viscosity on the shear rate, i.e., a clear non-Newtonian behavior. The required viscosity coefficients and other material parameters of *PHIC* are taken from the predictions of Doi's theory (Doi 1981) and Yang and Shine (1992), $\alpha_1=-2590$ Pa s, $\alpha_2=-3770$ Pa s, $\alpha_3=169$ Pa s, $\eta_c=3640$ Pa s and $\varepsilon_a\varepsilon_0=6.19\times10^{-9}$ N/V^2 (Yang and Shine 1992). Here we have also taken $K\sim10^{-12}$ N for the elastic constant and $l=4\times10^{-6}$ m for the separation distance between the plates.

The *ER* effect in simple shear flow may be exhibited by showing the variation of the spatially-averaged viscosity $\bar{\eta}(\bar{E})\equiv\int_{\zeta=-1/2}^{\zeta=1/2}\eta(\theta;\bar{E})\mathrm{d}\zeta$ as a function of the electric field strength (p), parametrized by the shear rate (m). The variation of this quantity as a function of the electric field is shown in Fig. 4. The viscosity tends to the zero shear rate asymptote as m tends to zero. The increase in the electric field strength gives rise to higher viscosity, since the director tends to be aligned with the electric field positioned normal to the flow direction, inducing higher resistance to flow. As in the case of Poiseuille flow (Rodríguez et al. 1999), the nematic solution exhibits a significant electrorheological effect, which is evidenced by the sharp increase in the viscosity $\bar{\eta}(\bar{E})$. The magnitude of the electrorheological effect diminishes as the flow strength rises, i.e., for larger values of m/p.

A very interesting effect is observed if we plot $\bar{\eta}$ as a function of m in a logarithmic scale. This is shown in Fig. 5 for high velocity gradients, where the viscosity decreases sharply for a given value of m. This critical velocity gradient depends on the magnitude of the field strength (p) in such a way that it increases for larger magnitudes of the electric field. The abrupt drop in the average viscosity is related to a negligible mean resistance to flow, which implies that the director orientation, on the average, is close to that of the fluid velocity. Since the viscosity depends entirely on the orientation angle θ, the

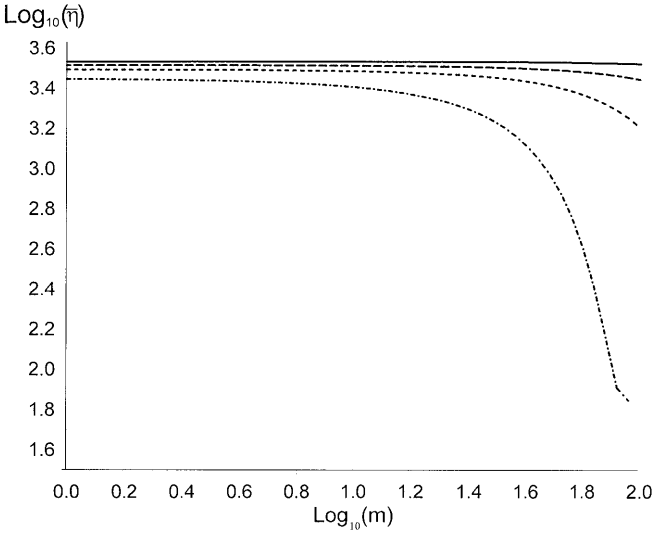

Fig. 5 Averaged viscosity $\bar{\eta}$ vs m parametrized by p. (—) $p=500$; (–) $p=200$; (···) $p=100$; (·–) $p=40$

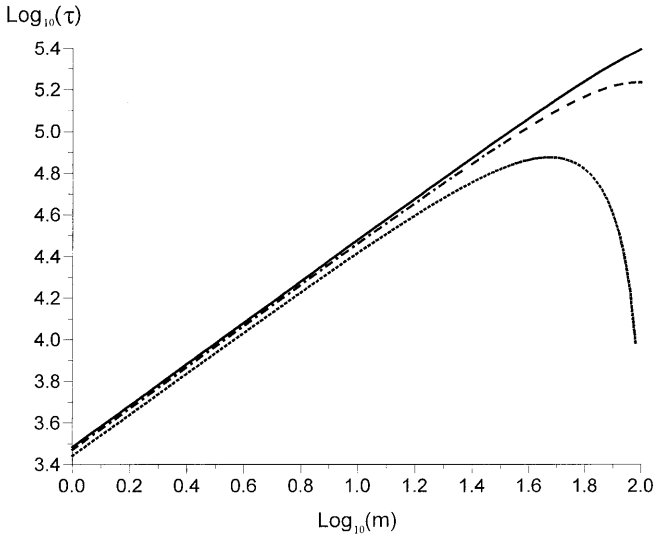

Fig. 6 Logarithmic plot of the stress τ vs m for different values of the electric field. (—) $p = 160$; (–) $p = 100$; (···) $p = 50$

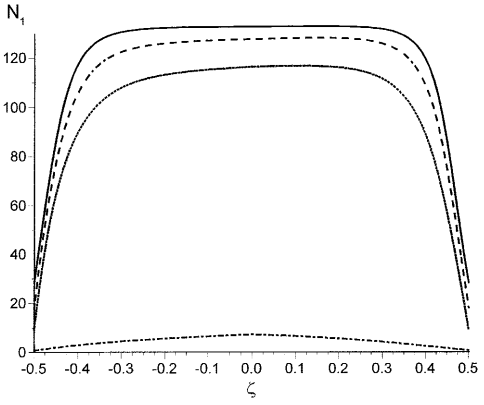

Fig. 7 First normal stress difference N_1 vs ζ for different values of m and p. (—) $m = 50$, $p = 160$; (–) $m = 100$, $p = 160$; (···) $m = 160$, $p = 160$; (·–·) $m = 10$, $p = 10$

flow is able to orient the director in the fluid velocity direction easier as the electric field strength decreases.

To estimate a typical value of the applied field, take, for instance, a saturation value $p = 800$ in the curve corresponding to $m/p = 0.1$ in Fig. 4. Then, from the above-mentioned definitions of p, q, and E_c, and using the values of K and ε_a corresponding to *PHIC*, we find that the critical field $E_c = 1.41 \times 10^3$ V/m and that the applied field is $E = 1.274 \times 10^5$ V/m$\sim 90E_c$. This shows that for rather small applied fields, a strong electrorheological effect may be produced in the cell.

Rheological properties

For flows that are simple variations of uniform shear flow, the stresses are uniform throughout the fluid and the material functions depend on the shear rate alone. In steady simple shear flows all transient stresses have died out and the steady stress depend on the shear rate $\dot{\gamma}$. The behavior of the stress τ vs m for different values of the electric field is shown in Fig. 6. First note that the initial slope of the curves is one, since the viscosity is constant for low values of m. At relatively high velocity gradients and for low electric fields, the stress reaches a maximum and shows a sharp drop at a critical velocity gradient, as also observed in the viscosity curves of Fig. 5. It is well known that fluids which exhibit a maximum in the stress may present a mechanical instability, since for a given stress there are two available values of the velocity gradient. In other words, regions of low and high viscosity co-exist for a given stress, implying that two average orientations also co-exist for the same stress. The hydrodynamic treatment by Carlsson (1984) in the absence of electric fields also allows for multiple values of the velocity gradient for a given stress. It is interesting that this effect induced by both flow and electric fields has been predicted by this model analytically; however, to our knowledge, there are no experimental data available to compare with.

In simple shear flow, the effects produced by the stresses generated during the reorientation process are qualitatively different to those obtained in pressure driven flows (Rodríguez et al. 1999). The first normal stress difference N_1 defined as $N_1 \equiv \sigma_{xx} - \sigma_{zz}$, for shear flow is given explicitly by

$$N_1[\theta(\zeta)] = -\lambda \frac{K}{l^2}\left[\sin 2\theta \frac{\mathrm{d}^2\theta}{\mathrm{d}\zeta^2} + \cos 2\theta \left(\frac{\mathrm{d}\theta}{\mathrm{d}\zeta}\right)^2 - q\cos^2\theta\right] . \tag{22}$$

Figure 7 shows the N_1 profile across the cell for different values of m and p. In contrast to the observed behavior of N_1 for plane Poiseuille flow where N_1 presents regions of negative values (Rodríguez et al. 1999), in simple shear this situation would only be possible with a strong electric field and weak flow, conditions which are not attainable within the present analytical approach which is restricted to values $m \sim p$. Notice that the N_1 profile is similar in form to that of the viscosity in Fig. 3. Most of the variation resides in the region close to the wall, increasing from zero at the wall and approaching a constant level in the central region of the cell. The value of N_1 at the center depends on the magnitude of the velocity gradient (m) and that of the electric field (p). For a fixed electric field, N_1 decreases at the center for higher velocity gradients, since the average director orientation tends to align itself with the velocity direction. Simultaneously, the width of the boundary layer increases due to a predominant orientation in the flow direction or parallel to the wall. Moreover, in the limit of very weak electric fields ($p = 10$), the curve at

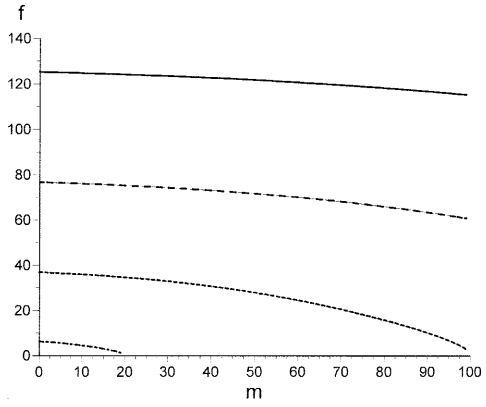

Fig. 8 The force $f \equiv \int_{-1/2}^{1/2} N_1[\theta(\zeta)]\mathrm{d}\zeta$ as a function of m parametrized by p. (—) $p = 160$; (–) $p = 100$; (···) $p = 50$; (·–·) $p = 10$

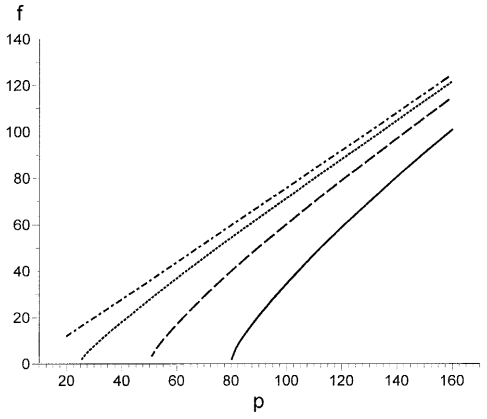

Fig. 9 f vs p parametrized by m. (—) m = 160; (–) m = 100; (···) m = 50; (·–·) $m = 1$

the bottom also reveals a predominant orientation with the flow, corresponding to negligible N_1.

In Fig. 8, the integration of the first stress difference profile over the whole cell renders the net force between the plates, $f \equiv \int_{-1/2}^{1/2} N_1(\theta(\zeta))\mathrm{d}\zeta$ as a function of the velocity gradient (m) for varying electric field strength (p). The net force increases with the electric field and remains almost constant with the velocity gradient for high values of p. The external field forces the average director orientation to be aligned perpendicular to the flow direction, producing a larger orientation gradient in the velocity gradient direction, and hence increasing the magnitude of the first normal stress difference. It is interesting to note that when $p = 50$, the magnitude of the force, f, decreases as the velocity gradient increases, and vanishes at $m = 100$. A vanishing N_1 is ascribed to a complete alignment of the director, on the average, with the flow direction. This situation agrees with results presented in Fig. 6 where, for $p = 50$, the shear stress presents a steep drop at around $m = 100$.

To investigate the regions where the force becomes negligible, Fig. 9 presents the variation of the force f as a function of the electric field strength p for several values of the velocity gradient m. It is very interesting to note from these curves that f becomes zero if and only if the ratio $m/p = 2$. By (17), this implies that the critical value of the Mason number, M_a^c, is

$$M_a^c = \frac{\nu_3}{2\gamma_1(1-\lambda)} \frac{\epsilon_0 \epsilon_a}{\epsilon_a \beta^2} \quad . \tag{23}$$

This critical ratio signals the limit of the electrorheological effect in such a way that when $M_c{}^a$ is exceeded, the *ER* vanishes. Our analytical approach allows us to calculate this critical value and express it in terms of material properties and flow parameters. It corresponds to a regime of complete alignment of the director with the velocity. Observation of Fig. 4 reveals that the magnitude of the average viscosity in the plateau region decreases as the ratio $m/p = 2$ is approached.

Carlsson and Sharp (1981) have also analyzed the stabilizing effect of an electric field on the shear flow of nematic liquid crystals. They showed that the presence of an ac field across the sample produces a stable boundary layer type of flow. They obtained explicit expressions for the flow alignment angle, the boundary layer and the relaxation time as functions of the electric field. Although their physical situation is essentially the same as the one considered in this work, there are important differences in the goals of both works. The solutions of the respective orientational equations for the final stationary state, our Eq. (8) and their Eq. (10), yield different orientational configurations because they neglect the influence of the walls. Therefore, a direct comparison is not feasible.

We conclude that the hydrodynamical model studied in this work showed that the reorientation induced by both, a simple shear flow and an external dc electric field on a nematic confined in a planar cell, may produce a dramatic increase in the viscosity known as the electrorheological effect. The analytical approach presented here allows for predictions of more than one possible value of the velocity gradient for a given value of the stress in the presence of an electric field. Also, our results provide the conditions under which the *ERE* vanishes due to complete alignment, on the average, of the director with the velocity field. These conditions depend on the ratio m/p and are such that for $p = m/2$, the viscosity shear stress and the first normal stress difference approach zero. In addition, at this particular value of the ratio m/p, the orientation of the director at the cell's center is the same for multiple values of m and p but keeping the fixed value $m/p = 2$.

Acknowledgments RFR and JAR gratefully acknowledge financial support from Grants DGAPA-UNAM IN105797 and CONACYT 400316-5-G25427E, Mexico.

References

Bender CM, Arszog MC (1978) Advanced mathematical methods for scientists and engineers. McGraw-Hill, New York

Block H, Kelly JP (1988) Electrorheology. J Phys D Appl Phys 21:1661–1668

Carlsson T (1984) Theoretical investigation of the shear flow of nematic liquid crystals with Leslie viscosity $\alpha_3 > 0$: hydrodynamic analogue of first order phase transitions. Mol Cryst Liq Cryst 104:307–334

de Gennes PG (1964) The physics of liquid crystals. Clarendon, Oxford

Khoo IC (1988) Nonlinear optics of liquid crystals. In: Wolf E (ed) Progress in optics, vol 26. North Holland, Amsterdam, and references therein

Miesowicz M (1935) Nature 17:261–267

Rodríguez RF, Reyes JA (1995) Waveguiding effect in a cell with a liquid crystalline core. Nonlin J Opt Phys Mat 4:943–958

Rodríguez RF, Reyes JA (1996) Propagation of optical fields in a planar liquid crystal wave guide. Mol Cryst Liq Cryst 282:287–296

Rodríguez RF, Camacho JF (1998) A model for electrorheology in polymeric liquid crystals. Rev Mex Fis 44:1859–1862

Rodríguez RF, Ortega P, Díaz-Uribe R (1996) Hydrodynamic effects in the optically-induced reorientation of nematic liquid crystals. Physica A 36:1079–1085

Rodríguez RF, Reyes JA, Manero O (1999) Model for the electrorheological effect in flowing polymeric nematics. J Chem Phys 110:8197–8204

San Miguel M, Sagués F (1987) Dynamics of transient pattern formation in nematic liquid crystals. Phys Rev A 36:1883–1890

Schlichting H (1968) Boundary layer theory. McGraw-Hill, New York

Tao R (ed) (1992) Electrorheological fluids. World Science Publishers, New York

Yang IK, Shine AD (1992) Electrorheology of a nematic poly(*n*-hexyl)isocyanate solution. J Rheol 36:1079–1104